Oncogene (2007) 26, 4243–4252

www.nature.com/onc

ORIGINAL ARTICLE

Global DNA methylation profiling reveals silencing of a secreted form of Epha7 in mouse and human germinal center B-cell lymphomas

DW Dawson[1], JS Hong[1], RR Shen[1], SW French[1], JJ Troke[1], Y-Z Wu[2], S-S Chen[2], D Gui[1], M Regelson[3], Y Marahrens[3], HC Morse III[4], J Said[1], C Plass[2] and MA Teitell[1,5]

[1]*Department of Pathology and Laboratory Medicine, David Geffen School of Medicine at UCLA, Los Angeles, CA, USA;* [2]*Molecular Virology, Immunology and Medical Genetics, Division of Human Cancer Genetics, The Ohio State University, Columbus, OH, USA;* [3]*Department of Human Genetics, The David Geffen School of Medicine at UCLA, Los Angeles, CA, USA;* [4]*Laboratory of Immunopathology, National Institute of Allergy and Infectious Disease, National Institutes of Health, Rockville, MD, USA and* [5]*Molecular Biology Institute, Institute for Stem Cell Biology and Medicine, California NanoSystems Institute, Institute for Cell Mimetic Studies and Jonsson Comprehensive Cancer Center, UCLA, Los Angeles, CA, USA*

Most human lymphomas originate from transformed germinal center (GC) B lymphocytes. While activating mutations and translocations of *MYC*, *BCL2* and *BCL6* promote specific GC lymphoma subtypes, other genetic and epigenetic modifications that contribute to malignant progression in the GC remain poorly defined. Recently, aberrant expression of the *TCL1* proto-oncogene was identified in major GC lymphoma subtypes. *TCL1* transgenic mice offer unique models of both aggressive GC and marginal zone B-cell lymphomas, further supporting a role for *TCL1* in B-cell transformation. Here, restriction landmark genomic scanning was employed to discover tumor-associated epigenetic alterations in malignant GC and marginal zone B-cells in *TCL1* transgenic mice. Multiple genes were identified that underwent DNA hypermethylation and decreased expression in *TCL1* transgenic tumors. Further, we identified a secreted isoform of *EPHA7*, a member of the Eph family of receptor tyrosine kinases that are able to influence tumor invasiveness, metastasis and neovascularization. *EPHA7* was hypermethylated and repressed in both mouse and human GC B-cell non-Hodgkin lymphomas, with the potential to influence tumor progression and spread. These data provide the first set of hypermethylated genes with the potential to complement *TCL1*-mediated GC B-cell transformation and spread.
Oncogene (2007) **26,** 4243–4252; doi:10.1038/sj.onc.1210211; published online 29 January 2007

Keywords: DNA methylation; B-cell lymphoma; TCL1

Correspondence: Dr MA Teitell, Department of Pathology and Laboratory Medicine, David Geffen School of Medicine at UCLA, 10833 LeConte Avenue, Mail Code 173216, Los Angeles, CA 90095-1732, USA.
E-mail: mteitell@ucla.edu
Received 31 August 2006; revised 3 November 2006; accepted 6 November 2006; published online 29 January 2007

Introduction

The TCL1 oncoprotein augments AKT activation and downstream signaling to promote cell proliferation and survival (Teitell, 2005). Dysregulated expression of *TCL1* is a frequent molecular alteration in non-Hodgkin lymphomas (NHLs) that arise by transformation of germinal center (GC) B-cells (Teitell *et al*., 1999; Narducci *et al*., 2000; Said *et al*., 2001). Supporting an etiologic role in transformation, dysregulated expression of *TCL1* in transgenic mouse B-cells throughout all stages of B-cell development promotes a spectrum of GC B-cell lymphoma subtypes that metastasize (Hoyer *et al*., 2002; Shen *et al*., 2006) or aggressive marginal zone-derived B-cell chronic lymphocytic leukemia (Bichi *et al*., 2002; Klein and Dalla-Favera, 2005; Yan *et al*., 2006). As *TCL1* transgenic (*TCL1-tg*) mice develop lymphomas only after a prolonged latency (Hoyer *et al*., 2002) and fail to develop lymphomas for up to 20 months when crossed into a GC-deficient background (Shen *et al*., 2006), additional molecular alterations within the GC appear to be essential for B-cell transformation. Chromosomal translocations and aneuploidy have been identified in transformed GC B-cells in *TCL1* transgenic mice (Shen *et al*., 2006), although it is unclear whether these genetic alterations drive or are merely reflective of the transformation process.

Cancer is associated with the accumulation of both genetic and epigenetic alterations (Esteller, 2003a; Herman and Baylin, 2003). DNA hypermethylation often correlates with inappropriate gene silencing and is well documented in primary human lymphomas and cell lines (Rush and Plass, 2002; Esteller, 2003b; Galm *et al*., 2006), and includes genes whose hypermethylation distinguish specific hematologic malignancies (Herman *et al*., 1997) or clinical outcome (Esteller *et al*., 2002). To date, altered DNA methylation in lymphoma has largely been addressed by direct candidate gene approaches. Therefore, it is likely that additional and important alterations in DNA methylation have yet to be described in lymphoma. Restriction landmark genomic scanning (RLGS) is a quantitative approach that distinguishes the

methylation status of over 2000 genetic loci and is particularly well suited for studying DNA methylation in the invariant genetic background of inbred mouse strains (Costello *et al*., 2002; Yu *et al*., 2005). In this paper, we used RLGS to identify 115 lymphoma-associated alterations in DNA methylation in our *TCL1* transgenic mouse model. We further investigated EphA7, a member of the Eph family of receptor tyrosine kinases. We found that normal lymphocytes express and secrete a truncated isoform of EphA7 instead of the full-length EphA7 receptor. *EPHA7* was selectively silenced by DNA hypermethylation in both mouse and human GC B-cell NHLs, with the potential to impact tumor growth and spread.

Results

DNA hypermethylation in TCL1-tg GC B-cell tumors

*Not*I—*Eco*RV–*Hin*fI RLGS profiles were generated on GC B-cell tumors, bulk non-neoplastic splenic tissue and sorted non-malignant splenic B or T cells from *TCL1-tg* mice (Hoyer *et al*., 2002) (Supplementary Figure 1). The use of methylation-sensitive *Not*I permitted the assessment of CpG methylation at the *Not*I landmark site. All results were referenced to a previously described master mouse RLGS profile that assigns numbers and map coordinates to each RLGS locus (Yu *et al*., 2005). Initial comparison between RLGS profiles generated on non-malignant sorted B-cells versus sorted T cells revealed only two differences (1D19 lost and 3C05 gained in T cells versus B-cells) for 1800 analysed RLGS loci (data not shown). In contrast, whole spleens had 59 differences out of 1800 analysed RLGS spots compared with either the sorted B- or T-cell profiles (data not shown), indicative of cell-specific methylation patterns distinct to non-B- and non-T-cell populations in the spleen (i.e., macrophages, vasculature or other stromal elements).

Our goal was to identify genes with the potential to suppress tumor growth or spread. Therefore, attention was focused on genes undergoing DNA hypermethylation in *TCL1-tg* B-cell tumors. Analysis was limited to those RLGS loci invariantly present in both the sorted B-cell profile and each of six separate profiles of *TCL1-tg* normal whole spleens. RLGS was performed on 11 *TCL1-tg* B-cell tumors, including six Burkitt-like/lymphoblastic lymphomas (LBL), three diffuse large B-cell lymphomas (DLBCL) and two marginal zone lymphomas (MZL) (Supplementary Table 1). Representative loci (4D57, 3C24 and 2C33) undergoing hypermethylation in one or more of the tumors are presented (Figure 1a). Of the 1741 RLGS loci analysed, 1626 loci were unaltered, whereas 115 loci were lost/hypermethylated in at least one tumor. The frequency of tumor-specific hypermethylation events ranged from 0.6 to 3.9% of the loci examined for each tumor, with a mean of 2.8% (Figure 1b). In the 11 tumors analysed, four loci were lost/hypermethylated in 10 tumors, three loci in nine tumors, seven loci in eight tumors, nine loci in seven tumors, nine loci in six tumors, 15 loci in five tumors, 18 loci in four tumors, 13 loci in three tumors, 16 loci in two tumors and 22 loci in only one tumor. Statistical analysis using a standard goodness-of-fit test indicated that DNA methylation in *TCL1-tg* B-cell tumors occurred in a nonrandom distribution ($P<0.0005$). Using previously described methodologies (Yu *et al*., 2005), 78 of the 115 loci undergoing hypermethylation were cloned and verified (data not shown). Verified sequences were analysed by BLAT (Kent, 2002) and are summarized in Table 1. Most identified loci (71/78) were in close proximity to known genes or mRNA sequences, 50 of 78 were located in the 5′ region of a gene and 69 of 78 occurred within canonical CpG islands.

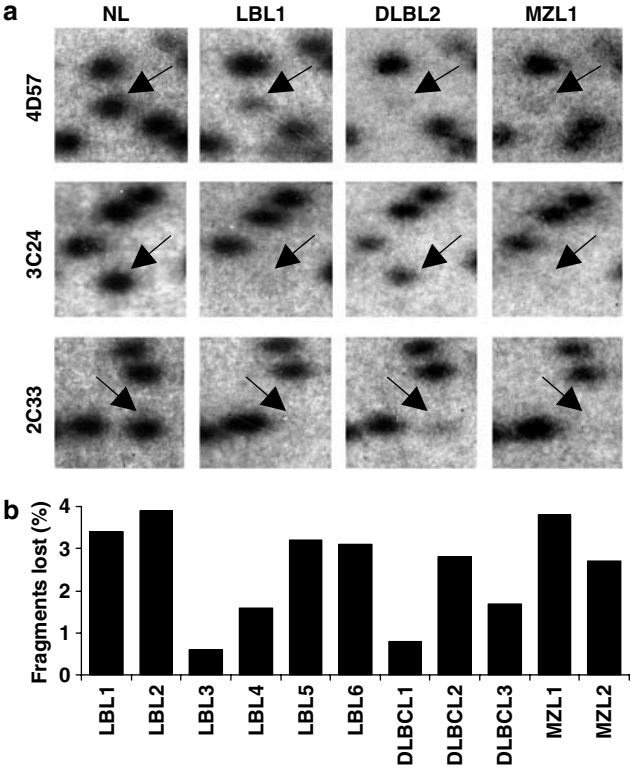

Figure 1 RLGS analysis for tumor-associated DNA hypermethylation. (**a**) Representative RLGS loci for non-malignant *TCL1-tg* mouse spleen (NL) and specified *TCL1-tg* splenic B-cell tumors. Arrows indicate specific RLGS loci (4D57, 3C24 and 2C33) lost/hypermethylated in one or more of the tumors. (**b**) Frequency of altered RLGS loci for each tumor is indicated.

Adoptive transfer of *TCL1-tg* LBL1 tumor cells into syngeneic mice results in the development of a phenotypically identical splenic lymphomas within 6 weeks (Hoyer *et al*., 2002). When the RLGS profiles of two of these daughter tumors (LBL1a and LBL1b) were compared with their LBL1 parental tumor, 1735 of the 1741 RLGS loci (99.6%) were identical (Table 1 and data not shown), indicating tumor-specific DNA methylation was stable for over 2 months (three weeks in culture and 6 weeks in syngeneic animals).

Table 1 DNA methylation patterns in lymphomas of TCL1-tg mice

Locus	LBL1	LBL1a*	LBL1b*	LBL2	LBL3	LBL4	LBL5	LBL6	DLBCL1	DLBCL2	DLBCL3	MZL1	MZL2	Chromosome position of *Not*I	Homology	GenBank accession number	Gene context	CpG island	# of tumors*
2C33	■	■	■	■	■	■	■	■		■		■	■	13:59285249	*Gas1*	NM_008086	5′ end	Yes	10
2F37	■	■	■	■	■	■	■	■	■	■		■	■	X:55,560,988	*Sox3*	NM_009237	5′ end	Yes	10
3F56	■	■	■	■	■	■	■	■	■	■	■	■	■	12:46,129,739	*Foxg1*	NM_008241	Body	Yes	10
4D57	■	■	■	■	■	■	■	■	■	■	■	■	■	4:28,999,648	*Epha7*	NM_010141	Body	Yes	10
2E37	■	■	■	■		■	■	■	■	■	■	■	■	17:66,614,500	mRNA	AK041052	5′ end	Yes	9
4G54	■	■	■	■	■	■		■	■	■	■	■	■	12:4,549,905	mRNA	AK122572	5′ end	Yes	9
2C09	■	■	■	■	■		■	■	■	■	■	■	■	4:98,631,630	*Foxd3*	NM_010425	5′ end	Yes	8
2G50	■	■	■		■	■	■	■	■	■	■	■	■	12:64,004,021	*Mamdc1*	NM_207010	5′ end	Yes	8
3D03	■	■	■	■	■	■	■	■	■	■	■	■	■	2:63,953,750	*Fign*	NM_021716	5′ end	Yes	8
2C14		■	■	■	■	■	■	■	■	■	■		■	X:94,421,625	-	-	-	Yes	7
3C09	■	■	■	■	■	■	■	■	■		■	■	■	9:88,074,776	*Tbx18*	NM_023814	Body	Yes	7
3F33	■	■	■	■	■	■	■		■	■	■	■	■	16:96,463,991	*Hmg14*	NM_008251	Body	Yes	7
4B16	■	■	■	■	■	■	■	■		■	■	■	■	2:68,327,187	*Stk39*	NM_016866	5′ end	Yes	7
4B22	■	■	■	■		■	■	■	■	■	■	■		5:130,774279	mRNA	BC066072	5′ end	No	7
4B42	■	■	■	■	■	■	■	■		■	■	■	■	3:62,005,545	mRNA	AK144976	5′ end	Yes	7
5B13	■	■	■	■	■	■	■	■		■	■	■	■	4:98,626,391	EST	AV377040	-	Yes	7
6D12	■	■	■	■	■	■	■	■	■	■	■	■		2:135,173,383	mRNA	AK020944	5′ end	Yes	7
3B46		■	■	■	■	■	■	■	■	■	■	■	■	2:68,326,347	*Stk39*	NM_016866	Body	Yes	6
3C10	■	■	■	■	■	■	■	■	■	■	■	■	■	2:84,412,897	*Zdhhc5*	NM_144887	5′ end	Yes	6
3C24	■	■	■	■	■	■	■	■	■	■	■	■	■	9:88,075,904	*Tbx18*	NM_023814	5′ end	Yes	6
3F09	■	■	■		■	■	■	■	■	■	■	■	■	3:44,840,447	*Pcdh10*	NM_011043	5′ end	Yes	6
4G73	■	■	■	■	■	■	■	■	■	■	■	■	■	8:90,392428	*Irx3*	NM_008393	Body	Yes	6
5B21	■	■	■	■	■	■	■	■		■	■	■	■	13:101,510,565	mRNA	AK032259	Body	Yes	6
5C30	■	■	■	■	■	■	■	■	■	■	■	■	■	13:59284349	*Gas1*	NM_008086	5′ end	Yes	6
1D14	■	■	■	■	■	■	■	■	■	■	■	■	■	10:67,589,894	*Egr2*	NM_010118	5′ end	Yes	5
1E19	■	■	■	■	■	■	■	■	■	■	■	■	■	4:13,670,306	*Mtg8*	AK032132	5′ end	Yes	5
2B07	■	■	■	■	■	■	■	■	■	■	■	■	■	3:17,385,384	*Bhlhb5*	NM_021560	5′ end	Yes	5
2F89	■	■	■	■	■	■	■	■	■	■	■	■	■	4:151,974,687	EST	BI990953	-	Yes	5
3B30	■	■	■	■	■	■	■	■	■	■	■	■	■	10:26,078,037	mRNA	AK021041	5′ end	Yes	5
4C11	■	■	■	■	■	■	■	■	■	■	■	■	■	16:14,160,631	mRNA	AK016529	Body	No	5
4D11		■	■	■	■	■	■	■	■	■	■	■	■	14:100,440,198	*Spry2*	NM_011897	5′ end	Yes	5
4D26	■			■	■	■	■	■	■		■			10:18,242,971	-	-	-	No	5
6C17	■	■	■		■	■	■	■	■	■	■	■	■	4:99,050,606	*Foxd3*	NM_010425	5′ end	Yes	5
6D39	■	■	■		■	■	■	■	■	■	■	■	■	4:28,932,608	*Epha7*	NM_010141	5′ end	Yes	5
6E07	■	■	■	■	■	■	■	■	■	■	■	■	■	6:61,148,968	mRNA	BC107398	5′ end	Yes	5
5D25	■	■	■	■	■	■	■	■	■	■	■	■	■	7:31,859,900	*Zfp537*	NM_172298	5′ end	Yes	5
1D16	■	■	■	■	■	■	■	■	■	■	■	■	■	7:31,861,437	*Zfp537*	NM_172298	5′ end	Yes	4
1F21		■	■	■	■	■	■	■	■	■	■	■	■	X:53,512,030	*Zic3*	NM_009575	5′ end	Yes	4
2C51				■	■	■	■	■	■	■	■	■	■	10:53,997,541	mRNA	AK015334	5′ end	Yes	4
2D07		■	■	■	■	■	■	■	■	■	■	■	■	9:49,836,621	*Ncam1*	NM_010875	Body	Yes	4
2D17			■	■	■	■	■	■	■	■	■	■	■	13:47,861,015	*Id4*	NM_031166	Body	No	4
2E38	■	■	■	■	■	■	■	■	■	■	■	■	■	2:59,016,731	*Pkp4*	NM_026361	Body	Yes	4
2G09				■	■	■	■	■	■	■	■	■	■	10:9,548,064	mRNA	AK087498	5′ end	Yes	4
2G14				■	■	■	■	■	■	■	■	■	■	6:23,885,534	*Cadps2*	NM_153163	5′ end	Yes	4
2G35				■	■	■	■	■	■	■	■	■	■	10:33,679,565	mRNA	AK169009	5′ end	Yes	4
3C27		■	■	■	■	■	■	■	■	■	■	■	■	2:74,353,577	*Evx2*	NM_007967	3′ end	Yes	4
3D67				■	■	■	■	■	■		■	■	■	4:130,910,515	*Oprd1*	NM_013622	3′ end	Yes	4
3F42	■	■	■	■	■	■	■	■	■	■	■	■	■	1:4,452,847	*Sox17*	NM_011441	3′ end	Yes	4
3F76		■	■	■	■	■	■	■	■	■	■	■	■	2:74,499,328	*Evx2*	BC061467	3′ end	Yes	4
3G102				■	■	■	■	■	■	■	■	■	■	2:144,624,936	*Slc24A3*	AF314821	5′ end	Yes	4
4B11	■	■	■	■		■	■	■	■	■	■	■	■	2:139,192,068	mRNA	AK077398	5′ end	Yes	4
5E24				■	■	■	■	■	■	■	■	■	■	10:28928152	mRNA	AK044134	5′ end	Yes	4
1F11				■	■	■	■	■	■	■	■	■	■	2:59,092,478	*Pkp4*	NM_026361	5′ end	Yes	3
2F12	■					■	■	■	■	■	■	■	■	18:51,332,715	mRNA	AK046456	5′ end	No	3
2F72							■	■	■	■	■	■	■	15:64,073,819	mRNA	BC011343	5′ end	Yes	3
2G48							■	■	■	■	■	■	■	12:106,919,086	*Tnfaip2*	NM_009396	Body	Yes	3
3D63					■	■	■	■	■	■	■	■	■	12:97,914,635	*Golga5*	NM_013747	5′ end	Yes	3
3G118							■	■	■	■	■	■	■	17:33,998,698	mRNA	AK138323	Body	Yes	3
4D49	■	■	■	■	■	■	■	■	■	■	■	■	■	13:24,749,912	*Vmp*	NM_009513	5′ end	No	3
5B27	■	■	■	■	■	■	■	■	■	■	■	■	■	10:28,927,390	mRNA	BC066079	Body	Yes	3
1F02				■	■	■	■	■	■	■	■	■	■	2:74,366,378	*Hoxd13*	NM_008275	5′ end	Yes	2
1F14	■	■	■	■	■	■	■	■	■	■	■	■	■	8:12371081	*Sox1*	NM_009233	5′ end	Yes	2
1G09				■	■	■	■	■	■	■	■	■	■	3:147,968,915	mRNA	AK142828	5′ end	Yes	2
2E09									■	■	■	■	■	1:154,165,496	-	-	-	Yes	2
2G05				■	■	■	■	■	■	■	■	■	■	5:148,345,311	mRNA	AK160904	5′ end	No	2
3C06	■	■	■	■	■	■	■	■	■	■	■	■	■	1:15,470,447	-	-	-	Yes	2
3G119									■	■	■	■	■	4:77,615,797	Ptprd	AK034145	5′ end	Yes	2
1C10									■	■	■	■	■	19:38,537,602	*Tbc1d12*		5′ end	Yes	1
1F30				■	■	■	■	■	■	■	■	■	■	11:8,576,675	mRNA	AK089717	Body	Yes	1
2D30	■	■	■	■	■	■	■	■	■	■	■	■	■	10:39,979406	-	-	-	No	1
2E10									■	■	■	■	■	6:24,898,673	mRNA	AK087465	5′ end	Yes	1
2F21							■	■	■	■	■	■	■	10:5,634,072	*Esr1*	AK036627	Body	Yes	1
3B15							■	■	■	■	■	■	■	13:31,173,603	*FoxC1*	NM_008592	5′ end	Yes	1
3D22				■	■	■	■	■	■	■	■	■	■	4:88,678261	*Cdkn2a*	NM_001040654	3′ end	No	1
3D28							■	■	■	■	■	■	■	12:71,498,554	*Tmem30b*	NM_178715	5′ end	Yes	1
3F14				■	■	■	■	■	■	■	■	■	■	2:140,136,707	mRNA	AK134694	5′ end	Yes	1
4D27	■								■	■	■	■	■	6:52,127,688	*Hoxa2*	NM_010451	5′ end	Yes	1
5D43				■	■	■	■	■	■	■	■	■	■	2:76,250,275	*Osbp16*	NM_145525	5′ end	Yes	1

Black squares denote RLGS fragments with decreased intensity of >50%. Tumor diagnosis and RLGS scoring is listed and includes two daughter tumors (LBL1a and b) from adoptive transfer of parental LBL1 tumor cells into syngeneic mice. *Not*I position lists chromosome followed by position based on UCSC BLAT search (Aug. 2005 Freeze). For gene context, 5′ end indicates location directly upstream or within first exon, 3′ end indicates location within the last exon of a gene, body indicates within gene itself excluding 5′ and 3′ ends. *Daughter tumors are excluded from calculations of total tumors showing fragment loss. EST, expressed sequence tag.

Validation of tumor-specific methylation detected by RLGS

The 4D57 locus localized to a CpG island within the gene *Epha7*, a member of the Eph family of receptor tyrosine kinases. Eph receptors and their ligands are capable of modulating immune cell function and development through diverse effects on receptor signaling, lymphocyte chemotaxis and adhesion (Wu and Luo, 2005). We chose to focus our attention on *Epha7* owing to its frequent hypermethylation (Table 1) and the potential to influence the growth and spread of aggressive *TCL1-tg* B-cell tumors. Although loss of an RLGS fragment is usually due to DNA hypermethylation (Costello *et al*., 2000), it may also result from point mutation or genomic deletion. Therefore, confirmatory Southern analysis was performed on 4D57 and was designed to assess the methylation status of two distinct *Not*I sites (Figure 2a). Increased methylation of one or both *Not*I sites was seen for all tumors, as demonstrated by protection from *Not*I enzymatic digestion (Figure 2b). When compared with non-malignant samples, the tumors showed a marked reduction in intensity of the 1.3 kb lower band (both *Not*I sites unmethylated) and an inverse increase in the 7.2 or 3.1 kb middle bands (owing to methylation of either the first or second *Not*I site, respectively) and 8.9 kb upper band (both *Not*I sites methylated).

To further validate RLGS results and obtain a detailed picture of DNA methylation across associated CpG islands, bisulfite sequencing was performed on the frequently lost 4D57, 3F09 and 5B13 loci (corresponding to the genes *Epha7*, *Pcdh10* and *Foxd3*, respectively). As the *Not*I site for 4D57 is located within the first intron of *Epha7*, bisulfite sequencing was also performed on a second region covering the 5′ untranslated region (UTR) and translational start site of *Epha7*. Both *Epha7* regions were highly methylated in tumors compared with non-malignant spleens or sorted B-cells (Figure 2c). Likewise, bisulfite sequencing of the *Pcdh10* promoter showed an average of 0.3 methylated CpG sites (1.7%) out of 17 CpG sites per clone for non-malignant spleen, and 10.8 methylated CpG sites (63%) out of 17 CpG sites per clone for tumor LBL1 (10 clones sequenced for each, data not shown). Bisulfite sequencing of the *Foxd3* promoter showed an average of 0.6 methylated CpG sites (5%) out of 12 CpG sites per clone for non-malignant spleen and 7.1 methylated CpG sites (59%) out of 12 CpG sites per clone for tumor LBL1 (10 clones sequenced for each, data not shown).

Silencing of specific hypermethylated genes in TCL1-tg tumors

To determine whether DNA methylation correlated with gene silencing, expression of *Epha7*, *Pcdh10* and

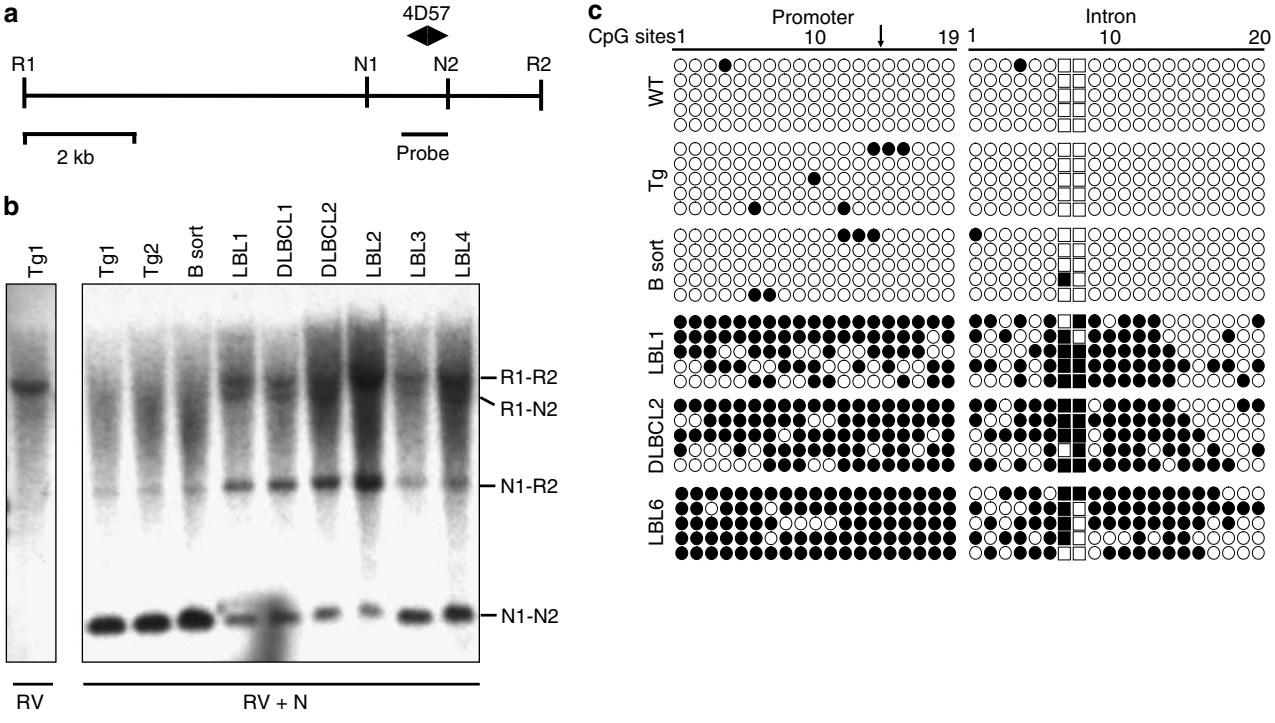

Figure 2 Validation of promoter methylation for *Epha7*. (**a**) Schematic diagram of genomic *Eco*RV–*Eco*RV fragment (sites R1 and R2) of murine *Epha7* containing two *Not*I sites (N1 and N2), as well as locations of the 4D57 *Not*I-*Hinf*I RLGS fragment and Southern probe. (**b**) Southern hybridization for *Epha7* on genomic DNA from non-malignant *TCL1-tg* spleens (Tg) or sorted B-cells (B sort) and malignant B-cell tumors. Digestions with *Eco*RV alone (first lane, RV) or in combination with methyl-sensitive *Not*I (remaining lanes, RV + N1) are indicated. Detected bands correspond to methylation of neither (N1–N2), both (R1–R2) or one of two *Not*I sites (R1–N2 or N2–R2). (**c**) Bisulfite sequence analysis of CpG islands located in the 5′ UTR and first intron of *Epha7*. Each row represents the sequence of an individual clone (open circle, unmethylated CpG site; filled circle, methylated site; squares, CpGs in the *Not*I site of the 4D57 locus; arrow, location of translational start site).

Foxd3 were analysed by real-time polymerase chain reaction (PCR) (Figure 3a–c). When compared with sorted non-malignant B-cells, tumors with DNA hypermethylation at 4D57 had a 3- to 34-fold reduction in *Epha7* expression, whareas one tumor (DLBCL1) without hypermethylation at 4D57 showed a less significant twofold reduction in expression (Figure 3a). Likewise, expression of *Pcdh10* and *Foxd3* in tumors was reduced 5–240-fold and 3–20-fold, respectively (Figure 3b and c). *Epha7* expression was found to be comparatively low in established murine pre-B (3–1) and mature B-cell lines (A20 and BAL17). To further validate the epigenetic regulation of *Epha7* expression, these cell lines or cultured primary *TCL1-tg* LBL1 cells were treated with the DNA demethylating agent 5-aza-2′-deoxycytidine (5-aza-dC) alone or in combination with the histone deacetylase inhibitor, trichostatin A (TSA). Dose-dependent induction of *Epha7* expression was seen in response to 5-aza-dC, with further substantial induction of *Epha7* with the addition of TSA (Figure 3d), thus supporting epigenetic silencing of *Epha7* in these malignant B-cells through combined DNA methylation and histone deacetylation.

Silencing and hypermethylation of EPHA7 in human B-cell lymphomas

We next evaluated *EPHA7* promoter methylation and gene expression in normal human lymphoid tissue and lymphomas. Primary human GC-NHL, including Burkitt lymphoma (BL), DLBCL, follicular lymphoma (FL) and MZL were chosen, paralleling lymphomas seen in *TCL1-tg* mice. Methylation-specific PCR (MS-PCR) analyses of DNA from normal human hyperplastic lymph nodes and tonsils demonstrated strong unmethylated bands and absent methylated bands for the *EPHA7* promoter (Figure 4a). Similar results were obtained with the human embryonic kidney cell line 293T, consistent with a previous report (Wang *et al*., 2005). In contrast, MS-PCR demonstrated methylation of the *EPHA7* promoter in 23 of the 31 informative patient lymphoma samples and the human pre-B-cell line, Nalm-6 (Figure 4a). By real-time PCR, the majority of lymphoma samples showed a 4–20-fold reduction in *EPHA7* expression when compared to DNA prepared from pooled hyperplastic lymph nodes, whereas each individual hyperplastic lymph node sample showed no significant reduction in *EPHA7* expression (Figure 4b). In some instances, *EPHA7* silencing did not appear to correlate with DNA hypermethylation (DLBL7, FL3, FL5, FL6 and MZL6), possibly owing to accompanying non-malignant lymphocytes in these samples. *EPHA7* expression did not show any correlation with *TCL1* expression status as determined by real-time PCR (data not shown). Robust induction of *EPHA7* expression in human B-cell lines Nalm-6 or Ramos following 5-aza-dC treatment alone or in combination with TSA provided additional support for epigenetic silencing of *EPHA7* in human B-cell neoplasms (Figure 4c).

Normal B and T lymphocytes express and secrete a truncated form of EphA7 protein

A previous study using semi-quantitative reverse transcription RT–PCR and Northern analysis shows that *EPHA7* is expressed by fetal bone marrow pro-B and

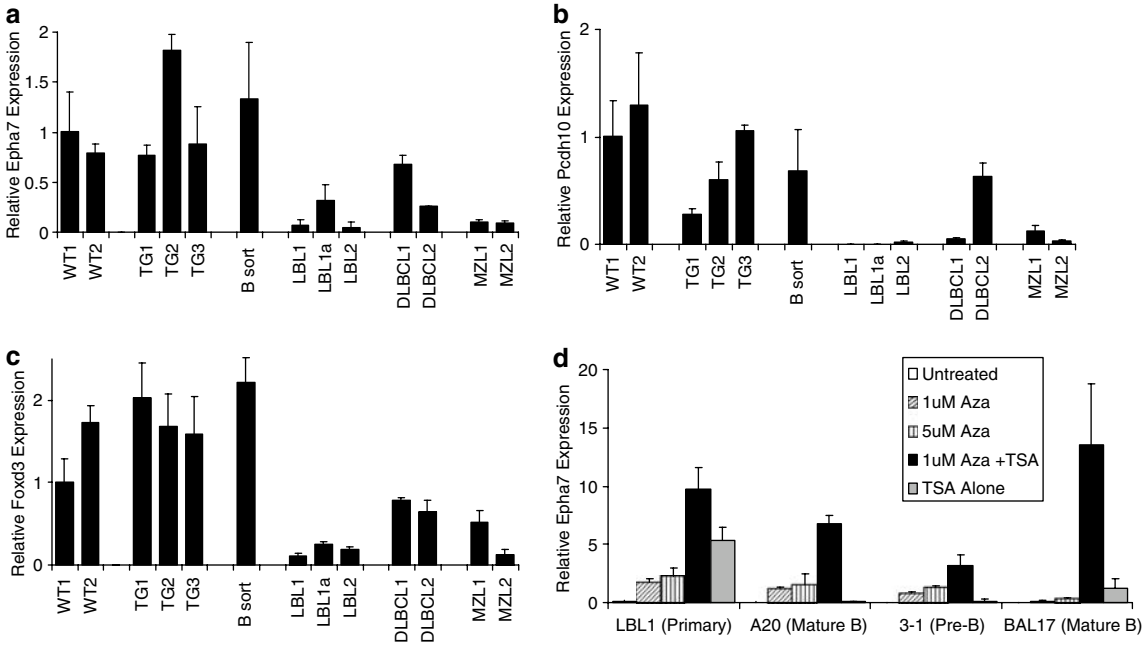

Figure 3 Gene silencing with increased promoter methylation in *TCL1-tg* lymphomas. Expression of *Epha7* (**a**), *Pcdh10* (**b**) or *Foxd3* (**c**) in non-malignant wild-type spleens (WT), *TCL1-tg* spleens (Tg) or sorted B-cells (B sort), as well as in *TCL1-tg* B-cell tumors (LBL, DLBCL and MZL), were quantified by real-time PCR. (**d**) Real-time PCR analysis of *Epha7* expression in cultured primary LBL1 tumor cells and murine B-cell lymphoma lines (A20, 3–1 and BAL17) before or after treatment with 5-aza-2′-deoxycytidine (Aza) and/or 100 nM TSA.

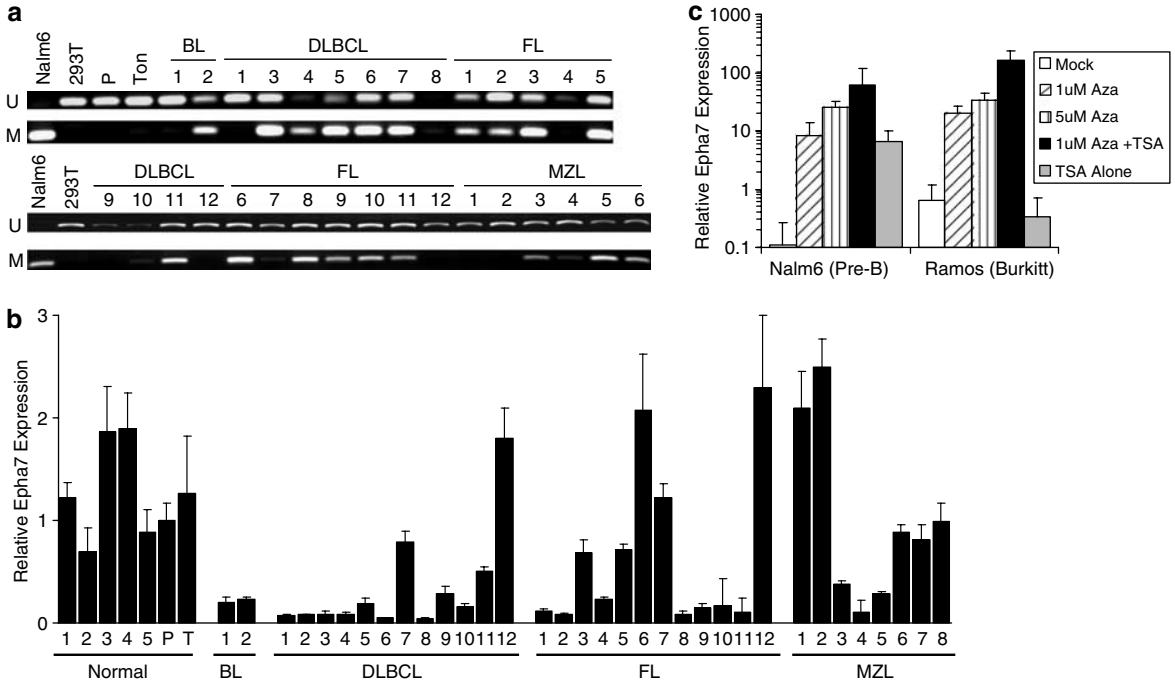

Figure 4 Promoter methylation and gene expression of *EPHA7* in human lymphomas. (**a**) Methyl-specific PCR was performed on Nalm-6 or 293T cell lines, a pool of 5 non-malignant hyperplastic human lymph nodes (P), reactive tonsil (T) and primary human GC-NHL samples including Burkitt lymphomas (BL), DLBCL, follicular lymphomas (FL) and MZL. Upper and lower bands correspond to PCR products amplified by primers specific to unmethylated (U) or methylated (M) CpG sites following bisulfite conversion. (**b**) *EPHA7* expression was measured by real-time PCR for the above samples, including each individual hyperplastic lymph node (N1–N5) from the pooled lymph nodes. (**c**) Real-time PCR analysis of *EPHA7* from Nalm-6 and Ramos before or after treatment with 5-aza-2′-deoxycytidine (Aza) and/or 100 nM TSA.

pre-B-cells, but not by more mature fetal B-lineage or adult B-lineage cells (Aasheim *et al*., 1997). Given the differences in primers used in this prior and our current study (covering the 3′ versus 5′ end of the full-length gene, respectively), we explored the possibility of an alternate *EPHA7* transcript and found a variant full-length 3.5-kb murine *Epha7* mRNA (*AK032973*) entry in GenBank. This alternate transcript encompasses the first five exons of full-length *Epha7* with read-through/termination in the fifth intron. It is predicted to encode a 451 amino acid, N-terminal truncated form of EphA7 protein comprising most of its extracellular domain, but lacking the transmembrane and intracellular domains (Figure 5a). PCR, using primers to the 5′ and 3′ ends of *AK032973*, was performed and successfully amplified a 3.5 kB product from murine splenic B-cell cDNA. This PCR product was cloned, sequenced and found to be identical to *AK032973* (data not shown).

EphA7 Western blots on whole cell lysates from sorted B and T cells from both mouse spleens and human tonsil failed to detect full-length EphA7 protein, as expected (Figure 5b). In contrast, Western blots on conditioned media (CM) from these same cells detected a 50-kDa band (Figure 5b), consistent with translation of the 3.5-kb variant transcript and secretion of the protein (which we now designate as EphA7-S) by the cells. Two different antibodies recognizing the extracellular domain of EphA7 detected the same 50-kDa protein in CM from sorted B or T cells from human tonsil (Figure 5c). A distinct 40-kDa band was also detected in CM from the human Burkitt line BJAB (Figure 5b). Although the exact identity of this 40-kDa band was not determined, a previous study reports multiple *EPHA7* transcripts (6.0, 4.4 and 2.0 kb) in BJAB cells by Northern blot, as well as nucleotide deletions in a sequenced *EPHA7* cDNA clone from the same cells (Aasheim *et al*., 1997).

Soluble EphA7 partially inhibits chemokine-induced B-cell migration

Eph/ephrin signaling is known to alter chemokine-induced lymphocyte chemotaxis (Sharfe *et al*., 2002), which prompted us to ask whether soluble EphA7 could influence B-lymphocyte chemotaxis in a transwell migration assay. To test this possibility, Nalm-6 B-cells were allowed to migrate to SDF-1α with or without preincubation with EphA7-Fc, a purified recombinant protein comprising the first 549 amino acids of the extracellular domain of EphA7. SDF-1α-induced migration was partially blocked by EphA7-Fc in a dose-dependent manner ($P<0.03$ for 0.1 or 1.0 μg/ml EphA7-Fc versus SDF alone, Student's *t*-test) (Figure 6a). Eph/ephrin signaling has also been shown to influence T-cell proliferation and apoptosis (Wu and Luo, 2005). However, flow cytometric studies with Annexin-V/propidium iodide (PI) staining showed that soluble

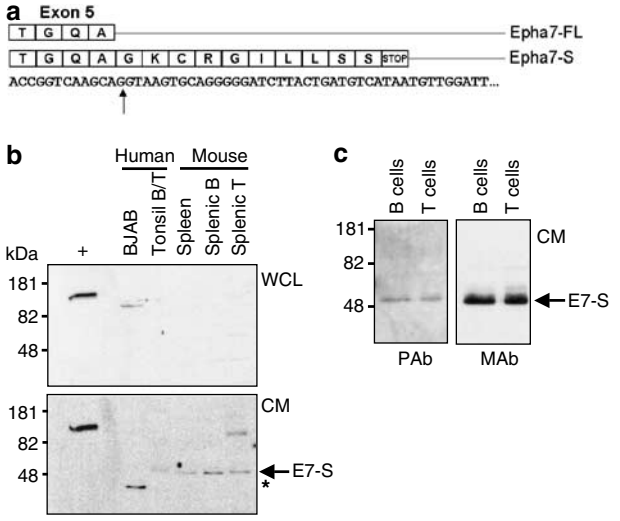

Figure 5 A variant transcript of *EPHA7* encodes EphA7-S, a soluble protein secreted by lymphocytes. (**a**) Nucleotide sequence and predicted amino acid sequence for full-length EphA7 (EphA7-FL) at the end of exon 5 (arrow-splice site) and for the variant transcript (EphA7-S) based on sequencing of a cDNA clone from murine splenic B-cells. (**b**) EphA7 expression was determined by Western blot (polyclonal antibody) on WCL or serum-free CM from the human B-cell line BJAB, sorted normal human tonsil B or T cells, normal murine whole splenocytes and sorted normal murine splenic B or T cells. WCL from Nalm-6 cells stably transfected with EphA7-FL served as a positive control (+). Arrow indicates EphA7-S (E7-S), asterisk indicates unidentified immunoreactive band in BJAB CM. (**c**) Western blots on CM from sorted normal human tonsil B or T cells using rabbit polyclonal (PAb) or rat monoclonal (MAb) antibodies against the extracellular domain of EphA7.

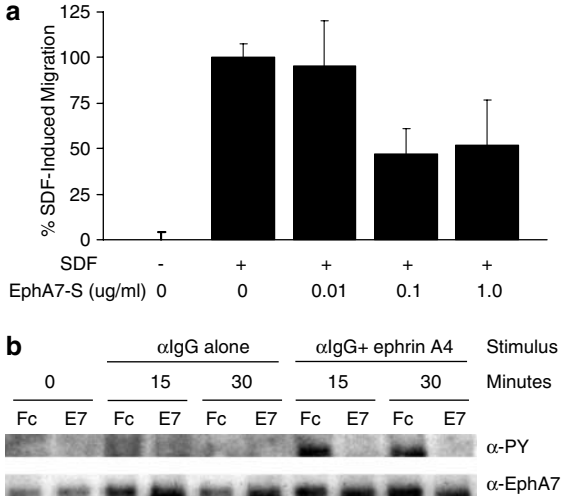

Figure 6 EphA7-S inhibits B-cell migration and ephrin ligand-induced EphA7 phosphorylation. (**a**) Nalm-6 B-cells (2×10^5 cells/well) were migrated for 2 h through a 5 μM pore membrane to recombinant SDF-1α (100 ng/ml), with or without pre-incubation with recombinant soluble EphA7-Fc (EphA7-S). Data is expressed as percentage of cells migrating to SDF-1α alone (typically 15–20% of input cells). All conditions were performed in triplicate. One of four representative experiments is shown. (**b**) EphrinA4-induced tyrosine phosphorylation of EphA7-FL expressing Nalm-6 cells was measured either in the presence of soluble EphA7-Fc or Fc alone. Cells were stimulated for indicated time, after which whole-cell lysates were immunoprecipitated with anti-EphA7 antibody followed by Western blot with anti-phosphotyrosine antibody, then re-probed with anti-EphA7 to verify equal total EphA7-FL in each well.

EphA7-Fc had no effect on apoptosis induced by IgM B-cell receptor ligation in the Ramos B-cell line (data not shown). Soluble EphA7-Fc also had no effect on the proliferation of Nalm-6 or Ramos B-cell lines at varying serum concentrations (1–10%), as measured by MTT assays (data not shown).

Soluble EphA7 blocks ephrin-A4-mediated activation of full-length EphA7 receptor

Eph receptors and their cognate membrane-bound ephrin ligands interact at sites of direct cell–cell contact to initiate bidirectional signaling in both receptor- and ligand-expressing cells (Holmberg and Frisen, 2002; Palmer and Klein, 2003; Pasquale, 2005). Binding of clustered ephrin-A ligands to the full-length EphA7 receptor results in phosphorylation of its intracellular kinase domain, initiating a signaling cascade that results in cell repulsion (Holmberg *et al*., 2000). This prompted us to ask whether soluble EphA7 can affect ephrinA ligand-induced activation of full-length Eph receptor. We used recombinant ephrin-A4 ligand to stimulate Nalm-6 cells stably transfected with full-length EphA7, either in the presence or absence of soluble EphA7. Ephrin-A4 effectively initiated EphA7 phosphorylation, and this phosphorylation was completely inhibited by co-incubation with soluble EphA7 (Figure 6b). Thus, soluble EphA7 is capable of disrupting full-length EphA7 receptor signaling initiated through ephrin ligand/Eph receptor clustering and activation.

Discussion

Using RLGS, we identified 115 DNA hypermethylation events in B-cell lymphomas from *TCL1-tg* mice. Between 0.6 and 3.9% of all RLGS loci were hypermethylated in each *TCL1-tg* lymphoma, a frequency comparable with previous RLGS studies of human leukemia and mouse hematologic malignancies (Rush *et al*., 2001, 2004; Yu *et al*., 2005). Certain tumors showed a much higher frequency of methylation compared to others in our sample set, suggesting that tumor progression for a subset of these lymphomas may be critically dependent on DNA hypermethylation, akin to the subsets of sporadic colorectal tumors with CpG Island Methylator Phenotype (Kondo and Issa, 2004).

The nonrandom distribution of DNA methylation identified by RLGS points to a characteristic methylation pattern for B-cell lymphomas and expands on prior work describing distinct patterns of methylation for leukemias or lymphomas (Esteller, 2003b). Recently, RLGS was used to study DNA hypermethylation in an *Il15* transgenic mouse model of T/natural killer (NK)

cell acute lymphoblastic leukemia (Yu *et al*., 2005). Many of the tumor-associated DNA hypermethylation changes detected in those leukemias are identical to those found in this study of GC B-cell lymphomas, suggesting that a common methylation profile may be shared by distinct hematologic malignancies. Common epigenetic alterations could act to reinforce a pre-existing lymphoid-specific developmental pattern of gene expression and/or serve to dysregulate specific subsets of genes with critical roles in lymphomagenesis.

TCL1-tg mice provide unique models of mature B-lymphoid tumorigenesis, distinct from most other genetic, viral or environmental manipulations of mice that typically give rise to more immature forms of lymphoma (Teitell, 2005). *TCL1* overexpression in the transgenic mice alone is insufficient for tumor development, indicating a need for additional critical molecular alterations. Therefore, genes that are targets of DNA hypermethylation and silencing in the *TCL1*-tg mouse model are potential tumor suppressor genes with importance in mouse and possibly human GC-NHL. Indeed, we were able to show parallel DNA hypermethylation and silencing of *EPHA7* in human GC-NHL. EphA7 is a member of the largest known subgroup of receptor tyrosine kinases, the Eph receptors, that interact with membrane-anchored ephrin ligands to initiate bidirectional signaling in both receptor- and ligand-expressing cells (Pasquale, 2005). Eph/ephrin signaling is dependent upon cell–cell interaction and influences a variety of biological processes including tissue morphogenesis, angiogenesis, neural plasticity, stem cell fate and immune cell function (Pasquale, 2005).

Altered expression of various ephrin ligands and Eph receptors occurs in a variety of cancers, with diverse effects on tumor growth, survival, metastasis and angiogenesis. *EPHA7* is highly upregulated in hepatocellular and lung carcinomas (Surawska *et al*., 2004). Conversely, *EPHA7* is a target of DNA hypermethylation and silencing in colorectal cancer (Wang *et al*., 2005). To our knowledge, our results are the first to show that *EPHA7* is a target of hypermethylation and silencing in mature B-cell lymphomas. Earlier reports indicate that *EPHA7* is not expressed in peripheral B lymphocytes (Aasheim *et al*., 1997; de Saint-Vis *et al*., 2003). However, our findings are not inconsistent with these prior studies, for RT–PCR primers used in prior studies would not have amplified the variant EphA7-S transcript described here. Of note, alternatively spliced mRNAs for murine *Epha7* are detected by Northern blot with a probe to the 5′ end of full-length *Epha7*, including a faint 3.5-kb transcript in mouse spleen (Ciossek *et al*., 1995). Likewise, a survey of normal human tissues by TaqMan PCR reveals *EPHA7* expression across a wide range of tissue types, with low to intermediate levels of *EPHA7* transcript found in spleen, using primers that cover the EphA7-S transcript (Hafner *et al*., 2004).

Our finding that murine and human peripheral lymphocytes secrete a truncated form of EphA7 is not without precedent. Aasheim *et al*. (2000) describe a splice variant of ephrinA4, which encodes a soluble protein secreted by B-cells and upregulated upon B-cell receptor ligation. Truncated Eph receptors retaining their ligand-binding capacity have been shown to block activation of the full-length receptor (Brantley *et al*., 2002; Cheng *et al*., 2003; Dobrzanski *et al*., 2004). Accordingly, we found that recombinant soluble EphA7 blocked ephrinA4-induced EphA7-FL phosphorylation *in vitro*. Given its promiscuity for various ephrin-A ligands (Gale *et al*., 1996), it is intriguing to hypothesize that EphA7 secreted by lymphocytes might act as a decoy to block EphA receptor-ephrinA ligand clustering and activation. In this manner, soluble EphA7 could influence lymphocyte chemotaxis and trafficking by inhibiting Eph/ephrin interaction and signaling between adjacent lymphocytes or other neighboring cells (i.e., dendritic cells, macrophages or endothelium). Indeed, we demonstrated that soluble EphA7 partially blocked the chemotaxis of Nalm-6 B-cells *in vitro*, presumably by disrupting endogenous EphA/ephrin-A signaling between these cells. Blocking soluble EphA7 secretion may abrogate its inhibitory activity on cell migration, thus enhancing tumor cell spread and recruitment of accessory cells able to promote tumor growth. As increased expression and activation of full-length Eph receptors may be a common feature of tumors with more aggressive or metastatic potential (Wimmer-Kleikamp and Lackmann, 2005), epigenetic silencing of *EPHA7* may serve to promote tumor aggressiveness by eliminating the inhibitory activity of secreted EphA7 on tumor-promoting EphA receptor signaling.

Materials and methods

Tumor samples and cell lines

The *TCL1-tg* mouse model has been described (Hoyer *et al*., 2002) and is covered in greater detail in Supplementary methods. Human tissue and tumors were obtained from the UCLA Tissue Procurement Core Laboratory in accordance with institutional guidelines and Institutional Review Board (IRB) approval. Nalm-6 were provided by D Rawlings, whereas all other human and mouse lines were obtained from the American Type Culture Correction (ATCC). LBL1 cells were cultured from a *TCL1-tg* mouse with lymphoblastic lymphoma (Hoyer *et al*., 2002). For CM, cells were rinsed twice in phosphate-buffered saline (PBS) and allowed to condition serum-free media for 24 h, which was concentrated 100-fold by Centriprep filter centrifugation (10 kDa cutoff, Millipore, Billerica, MA, USA). See Supplementary Information for details regarding mouse and human lymphocyte isolations, chemotaxis assays and drug treatments.

Nucleic acid isolation and RLGS

RNA and DNA were isolated using Trizol reagent (Invitrogen, Carlsbad, CA, USA). DNA for RLGS was isolated from snap-frozen mouse spleens and RLGS was performed as described previously (Costello *et al*., 2002). Tumor RLGS profiles were analysed by superimposing films against a background profile generated on sorted, non-malignant splenic B-cells (see below). Spot loss or decreased intensity of at least 50% was scored as 'spot loss' or hypermethylation event.

Southern blot
Genomic DNA (10 μg/sample) was digested with *Eco*RV and *Not*I, separated on a 0.8% agarose gel and transferred to positively charged nylon membrane. The Southern probe was generated by digesting the 4D57 RLGS clone with *Not*I and *Sca*I to generate an 872 bp *Epha7* genomic fragment, which was then random-prime labeled with $\alpha[P^{32}]$dCTP.

Real-time PCR
For first strand cDNA synthesis, 2 μg of total RNA was reverse-transcribed with random hexamer primers using the Superscript First Strand Synthesis System (Invitrogen). SYBR green real-time quantitative PCR assays were performed using an Applied Biosystems (Foster City, CA, USA) 7700 sequence detector. Amplification reactions were carried out in 20 μl with cDNA, 300 nM forward/reverse primers and 10 μl of 2 $\times$ SYBR green master mix. Reaction parameters were 50°C for 5 s, 95°C for 15 min, followed by 40 cycles of 95°C for 15 s, 60°C for 30 s and 72°C for 30 s. Samples were analysed in parallel for *36B4* expression, which served as the normalization control. The human primers were: *hEPHA7* forward (F) (5′-TACCCCGATACGAACATACCAG-3′), *hEPHA7* reverse (R) (5′-AGGAAGACTGTTACAATCCCTCA-3′), *h36B4* F (5′-TCG-AACACCTGCTGGATGAC-3′) and *h36B4* R (5′-CCC GCTGCTGAACATGCT-3′). The murine primers were *mEPHA7* F (5′-TCAAACTCGGTTCCCTTCGTGGAT-3′), *mEPHA7* R (5′-AGA-AATCCAGTTAGTCCGCAGCCA-3′), *m36B4* F (5′-AGATGCAGCAGATCCGCAT-3′) and *m36B4* R (5′-GTTCTTGCCCATCAGCACC-3′). Other primer sequences are available upon request.

Bisulfite sequencing and MS-PCR
For bisulfite sequencing, PCR reactions of 35 cycles were performed (primers available upon request) on sodium bisulfite-treated DNA. PCR products were separated on agarose gels, extracted and cloned into pCR2.1Topo vector (Invitrogen). Individual clones were then sequenced. MS-PCR for the human *EPHA7* promoter was performed as described previously (Wang *et al*., 2005). Primer sets amplified a 229-bp product located at the same genomic site (forward primers located at −432 to −413 and reverse primers located at −223 to −204, relative to the translational start site).

Western blot and phosphorylation analysis
For EphA7 Western blots, CM (10 μg per sample) or RIPA whole cell lysates (50 μg per sample) were resolved by sodium dodecyl sulfate–polyacrylamide gel electrophoresis (SDS–PAGE), transferred to membranes, incubated overnight with 1:1000 anti-Epha7 antibody (rabbit polyclonal K16, Santa Cruz (Santa Cruz, CA, USA); or rat monoclonal clone 88712, R&D Systems (Minneapolis, MN, USA)) and then 1 h with 1:5000 horse radish peroside (HRP)-linked secondary antibody (Jackson Immunoresearch, West Grove, PA, USA). For phosphotyrosine analysis, FL-EphA7-expressing Nalm-6 cells (2.5×10^6 cells/condition, see supplemental methods for details regarding generation of FL-EphA7-expressing Nalm-6 cells) were stimulated at 37°C for the indicated times with anti-IgG-crosslinked recombinant human ephrin-A4 (amino acids 1–171 of ephrin-A4 fused to the Fc region of human IgG_1, R&D Systems) or anti-IgG alone in the presence of soluble recombinant EphA7 protein (amino acids 1–549 of the extracellular domain of mouse EphA7 fused to Fc) or recombinant Fc itself (R&D Systems). All proteins and anti-IgG were used at final concentrations of 40 μg/ml. Cells were rinsed 2 $\times$ in cold PBS, lysed in radio immunoprecipitation assay (RIPA) buffer and lysates (equalized for volume and protein concentration) were incubated overnight at 4°C with monoclonal anti-Epha7 antibody. Next, samples were bound to Protein G-Plus agarose beads for 2 h, washed thrice in RIPA buffer, boiled, resolved by SDS–PAGE and immunoblotted with anti-phosphotyrosine antibody (4G10, Upstate Biotechnology, Billerica, MA, USA). Equal immunoprecipitation of Epha7 protein was verified by reprobing the same blot with anti-Epha7 antibody.

Acknowledgements

This work was supported by the NIH Grants T32CA009120 (DWD), T32A107126 (RRS) T32CA09056 (SWF), HD041451 (YM), PNEY018228, R01CA90571, R01CA107300 and R01GM073981 (MAT), by the Margaret E Early Medical Research Trust, by CMISE, a NASA URETI Institute (NCC 2-1364) (MAT) and by the Intramural Research Program of the NIH, National Institute of Allergy and Infectious Diseases (HCM). MAT is a Scholar of the Leukemia and Lymphoma Society.

References

Aasheim HC, Munthe E, Funderud S, Smeland EB, Beiske K, Logtenberg T. (2000). A splice variant of human ephrin-A4 encodes a soluble molecule that is secreted by activated human B lymphocytes. *Blood* **95**: 221–230.

Aasheim HC, Terstappen LW, Logtenberg T. (1997). Regulated expression of the Eph-related receptor tyrosine kinase Hek11 in early human B lymphopoiesis. *Blood* **90**: 3613–3622.

Bichi R, Shinton SA, Martin ES, Koval A, Calin GA, Cesari R *et al*. (2002). Human chronic lymphocytic leukemia modeled in mouse by targeted TCL1 expression. *Proc Natl Acad Sci USA* **99**: 6955–6960.

Brantley DM, Cheng N, Thompson EJ, Lin Q, Brekken RA, Thorpe PE *et al*. (2002). Soluble Eph A receptors inhibit tumor angiogenesis and progression *in vivo*. *Oncogene* **21**: 7011–7026.

Cheng N, Brantley D, Fang WB, Liu H, Fanslow W, Cerretti DP *et al*. (2003). Inhibition of VEGF-dependent multistage carcinogenesis by soluble EphA receptors. *Neoplasia* **5**: 445–456.

Ciossek T, Millauer B, Ullrich A. (1995). Identification of alternatively spliced mRNAs encoding variants of MDK1, a novel receptor tyrosine kinase expressed in the murine nervous system. *Oncogene* **10**: 97–108.

Costello JF, Fruhwald MC, Smiraglia DJ, Rush LJ, Robertson GP, Gao X *et al*. (2000). Aberrant CpG-island methylation has non-random and tumour-type-specific patterns. *Nat Genet* **24**: 132–138.

Costello JF, Smiraglia DJ, Plass C. (2002). Restriction landmark genome scanning. *Methods* **27**: 144–149.

de Saint-Vis B, Bouchet C, Gautier G, Valladeau J, Caux C, Garrone P. (2003). Human dendritic cells express neuronal Eph receptor tyrosine kinases: role of EphA2 in regulating adhesion to fibronectin. *Blood* **102**: 4431–4440.

Dobrzanski P, Hunter K, Jones-Bolin S, Chang H, Robinson C, Pritchard S *et al*. (2004). Antiangiogenic and antitumor efficacy of EphA2 receptor antagonist. *Cancer Res* **64**: 910–919.

Esteller M. (2003a). Cancer epigenetics: DNA methylation and chromatin alterations in human cancer. *Adv Exp Med Biol* **532**: 39–49.

Esteller M. (2003b). Profiling aberrant DNA methylation in hematologic neoplasms: a view from the tip of the iceberg. *Clin Immunol* **109**: 80–88.

Esteller M, Gaidano G, Goodman SN, Zagonel V, Capello D, Botto B *et al*. (2002). Hypermethylation of the DNA repair gene *O*(6)-methylguanine DNA methyltransferase and survival of patients with diffuse large B-cell lymphoma. *J Natl Cancer Inst* **94**: 26–32.

Gale NW, Holland SJ, Valenzuela DM, Flenniken A, Pan L, Ryan TE *et al*. (1996). Eph receptors and ligands comprise two major specificity subclasses and are reciprocally compartmentalized during embryogenesis. *Neuron* **17**: 9–19.

Galm O, Herman JG, Baylin SB. (2006). The fundamental role of epigenetics in hematopoietic malignancies. *Blood Rev* **20**: 1–13.

Hafner C, Schmitz G, Meyer S, Bataille F, Hau P, Langmann T *et al*. (2004). Differential gene expression of Eph receptors and ephrins in benign human tissues and cancers. *Clin Chem* **50**: 490–499.

Herman JG, Baylin SB. (2003). Gene silencing in cancer in association with promoter hypermethylation. *N Engl J Med* **349**: 2042–2054.

Herman JG, Civin CI, Issa JP, Collector MI, Sharkis SJ, Baylin SB. (1997). Distinct patterns of inactivation of p15INK4B and p16INK4A characterize the major types of hematological malignancies. *Cancer Res* **57**: 837–841.

Holmberg J, Clarke DL, Frisen J. (2000). Regulation of repulsion versus adhesion by different splice forms of an Eph receptor. *Nature* **408**: 203–206.

Holmberg J, Frisen J. (2002). Ephrins are not only unattractive. *Trends Neurosci* **25**: 239–243.

Hoyer KK, French SW, Turner DE, Nguyen MT, Renard M, Malone CS *et al*. (2002). Dysregulated TCL1 promotes multiple classes of mature B-cell lymphoma. *Proc Natl Acad Sci USA* **99**: 14392–14397.

Kent WJ. (2002). BLAT – the BLAST-like alignment tool. *Genome Res* **12**: 656–664.

Klein U, Dalla-Favera R. (2005). New insights into the phenotype and cell derivation of B-cell chronic lymphocytic leukemia. *Curr Top Microbiol Immunol* **294**: 31–49.

Kondo Y, Issa JP. (2004). Epigenetic changes in colorectal cancer. *Cancer Metastasis Rev* **23**: 29–39.

Narducci MG, Pescarmona E, Lazzeri C, Signoretti S, Lavinia AM, Remotti D *et al*. (2000). Regulation of TCL1 expression in B- and T-cell lymphomas and reactive lymphoid tissues. *Cancer Res* **60**: 2095–2100.

Palmer A, Klein R. (2003). Multiple roles of ephrins in morphogenesis, neuronal networking, and brain function. *Genes Dev* **17**: 1429–1450.

Pasquale EB. (2005). Eph receptor signalling casts a wide net on cell behaviour. *Nat Rev Mol Cell Biol* **6**: 462–475.

Rush LJ, Dai Z, Smiraglia DJ, Gao X, Wright FA, Fruhwald M *et al*. (2001). Novel methylation targets in *de novo* acute myeloid leukemia with prevalence of chromosome 11 loci. *Blood* **97**: 3226–3233.

Rush LJ, Plass C. (2002). Alterations of DNA methylation in hematologic malignancies. *Cancer Lett* **185**: 1–12.

Rush LJ, Raval A, Funchain P, Johnson AJ, Smith L, Lucas DM *et al*. (2004). Epigenetic profiling in chronic lymphocytic leukemia reveals novel methylation targets. *Cancer Res* **64**: 2424–2433.

Said JW, Hoyer KK, French SW, Rosenfelt L, Garcia-Lloret M, Koh PJ *et al*. (2001). TCL1 oncogene expression in B-cell subsets from lymphoid hyperplasia and distinct classes of B-cell lymphoma. *Lab Invest* **81**: 1–10.

Sharfe N, Freywald A, Toro A, Dadi H, Roifman C. (2002). Ephrin stimulation modulates T cell chemotaxis. *Eur J Immunol* **32**: 3745–3755.

Shen RR, Ferguson DO, Renard M, Hoyer KK, Kim U, Hao X *et al*. (2006). Dysregulated TCL1 requires the germinal center and genome instability for mature B-cell transformation. *Blood* **108**: 1991–1998.

Surawska H, Ma PC, Salgia R. (2004). The role of ephrins and Eph receptors in cancer. *Cytokine Growth Factor Rev* **15**: 419–433.

Teitell M, Damore MA, Sulur GG, Turner DE, Stern MH, Said JW *et al*. (1999). TCL1 oncogene expression in AIDS-related lymphomas and lymphoid tissues. *Proc Natl Acad Sci USA* **96**: 9809–9814.

Teitell MA. (2005). The TCL1 family of oncoproteins: co-activators of transformation. *Nat Rev Cancer* **5**: 640–648.

Wang J, Kataoka H, Suzuki M, Sato N, Nakamura R, Tao H *et al*. (2005). Downregulation of EphA7 by hypermethylation in colorectal cancer. *Oncogene* **24**: 5637–5647.

Wimmer-Kleikamp SH, Lackmann M. (2005). Eph-modulated cell morphology, adhesion and motility in carcinogenesis. *IUBMB Life* **57**: 421–431.

Wu J, Luo H. (2005). Recent advances on T-cell regulation by receptor tyrosine kinases. *Curr Opin Hematol* **12**: 292–297.

Yan XJ, Albesiano E, Zanesi N, Yancopoulos S, Sawyer A, Romano E *et al*. (2006). B-cell receptors in TCL1 transgenic mice resemble those of aggressive, treatment-resistant human chronic lymphocytic leukemia. *Proc Natl Acad Sci USA* **103**: 11713–11718.

Yu L, Liu C, Vandeusen J, Becknell B, Dai Z, Wu YZ *et al*. (2005). Global assessment of promoter methylation in a mouse model of cancer identifies ID4 as a putative tumor-suppressor gene in human leukemia. *Nat Genet* **37**: 265–274.

Supplementary Information accompanies the paper on the Oncogene website (http://www.nature.com/onc).